J. Nucl. Phys. Mat. Sci. Rad. A. Vol. 8, No. 2 (2021), pp.161–168

CHITKARA

Journal of Nuclear Physics, Material Sciences, Radiation and Applications

Journal homepage: https://jnp.chitkara.edu.in/

Charged Lepton Masses as a Possible CPV Source

J.E. Barradas-Guevara[1], O. Félix-Beltrán[2*] and F. González-Canales[2]

[1]*Fac. de Ciencias Físico Matemáticas, Benemérita Universidad Autónoma de Puebla, Apdo. Postal 1152, Puebla, Pue. 72000, México*

[2]*Fac. de Ciencias de la Electrónica, Benemérita Universidad Autónoma de Puebla, Apdo. Postal 542, Puebla, Pue. 72000, México*

[*]olga.felix@correo.buap.mx (Corresponding Author)

ARTICLE INFORMATION

Received: September 18, 2020
Accepted: January 23, 2021
Published Online: February 10, 2021

Keywords:
Neutrino masses, CP violation, Tri-bi-Maximal

DOI: 10.15415/jnp.2021.82021

ABSTRACT

We realize a model-independent study of the so-called Tri-Bi-Maximal pattern of leptonic flavor mixing. Different charged lepton mass matrix textures are studied. In particular, we are interested in those textures with a minimum number of parameters and that are able to reproduce the current experimental data on neutrino oscillation. The textures studied here form an equivalent class with two texture zeros. We obtain a Tri-Bi-Maximal pattern deviation in terms of the charged leptons masses, leading to a reactor angle and three CP violation phases non-zero. These lastest are one CP violation phase Dirac-like and two phases Majorana-like. Also, we can test the phenomenological implications of the numerical values obtained for the mixing angles and CP violation phases, on the neutrinoless double beta decay, and in the present and upcoming experiments on long-base neutrino oscillation, such as T2K, NOvA, and DUNE.

1. Introduction

Detecting neutrinos requires the use of very large and precise devices, in addition to avoiding interference caused by other natural phenomena. Therefore, experiments to detect neutrinos must be installed deep within the Earth or Sea [1, 2]. Some examples of experiments located in mines are Homestake [3], Super-Kamiokande [4], and SNO [5, 6], while the ANTARES experiment is located in the depths of the Mediterranean Sea [7]. In the aforementioned experiments, the quantum mechanical phenomenon of neutrino oscillation can be detected. This phenomenon consists in that the flavor of the neutrino (electron neutrino ν_e, muon neutrino ν_μ, and tau neutrino ν_τ) changes as it travels through space, therefore the flavor of the neutrino that is emitted at the source is not necessarily the same as detected in the experiment. Furthermore, to have this flavor oscillation it is necessary that the neutrinos have a non-zero mass [2].

In the theoretical framework of the Standard Model (SM), which governs the dynamics of fundamental particles and their interactions [8], there are three massless neutrinos, which are treated as Dirac particles, and these neutrinos have the flavors ν_e, ν_μ, and ν_τ [1, 2]. However, a well-established fact is that from solar, atmospheric, and reactor neutrino oscillation experiments, the neutrino changes flavor as it travels due to its small mixing of mass and flavor [9]. So, this is clear evidence for physics beyond SM.

One of the main characteristics of neutrinos is to have a zero-electric charge, which is why, in the context of Quantum Field Theory, these particles can be represented as Dirac or Majorana particles. Thus, neutrinos apart from being chameleonic as they change their flavor while traveling from the source to the detector, also have an identity problem. In other words, until now, if the existing experimental data are considered, the nature of the neutrinos cannot be determined. However, in minimum extensions of the SM, considering neutrinos as Majorana particles explains very well the smallness of their mass [10]. The smallness in the neutrino mass scale is well explained by the seesaw mechanism, which links it to a new physical scale in nature [9].

The neutrino flavor mixing exhibits a very interesting pattern, in which two mixing angles from a three-flavor scenario appear to be maximum, while the third is still very small. Different lepton flavor mixing schemes such as Tri-Bi-Maximum (TBM) [11], Bi-maximum (BM) [12], and democratic mixing (DC) [13] have been explored in order to explain the experimental data on the neutrino oscillations. The leptonic flavor mixing scenarios TBM, BM, and DC have the same prediction for the reactor

ISSN No.: 2321-8649(Print) ISSN No.: 2321-9289(Online); Registration No. : CHAENG/2013/51628

mixing angle, $\theta_{13} = 0$ [11-13], whereas Atmospheric mixing angle is $\theta_{23} = 45^{\circ}$ for BM and TBM scenarios, and DC takes the value $\theta_{23} = 54.7^{\circ}$. The solar mixing angle is maximum, $\theta_{12} = 45^{\circ}$ for BM and DC, whereas for TBM scenario takes the value $\theta_{23} = 35.3^{\circ}$. In 2011, the long-baseline experiment T2K [14] observing the events of the transition probability $\nu_{\mu} \to \nu_{e}$, reported the following reactor angle values $5^{\circ} < \theta_{13} < 16^{\circ}$ for a Normal Hierarchy (NH, $\mathrm{m}_{\nu 3} > \mathrm{m}_{\nu 2} > \mathrm{m}_{\nu 1}$), and $5.8^{\circ} < \theta_{13} < 16.8^{\circ}$ for an Inverted Hierarchy (IH, $\mathrm{m}_{\nu 2} > \mathrm{m}_{\nu 1} > \mathrm{m}_{\nu 3}$), in the mass spectrum. However, the Daya Bay experiment presented the first conclusive results to have a reactor angle different to zero [15]. The mixing angle value θ_{13} at 90% C.L. is $\sin^2 2\theta_{13} = 0.092 \pm 0.016(stat) \pm 0.05(syst)$. From the previous results, it is evident that the BM, TBM, and DC scenarios cannot be considered at their nominal value. Therefore, they must be analyzed to determine possible deviations from them.

In Table 1 we show the last results of a global fit of neutrino oscillation data in the simplest three-neutrino framework. From these values, one can easily conclude that neutrino physics is in its precision stage with respect to its fundamental parameter determination. However, the CPV phase factors are in their first stage of predicting values, since only for the phase Dirac-like there exists a value range obtained from the global fit of neutrino data. But in the case when the neutrino is a Majorana particle, the other two CPV phases associated with the effective mass in the neutrinoless double beta decay, do not have experimental evidence for obtaining their values.

Table 1: Numerical values of the parameter related with neutrino oscillations, obtained on global fit [16]. Here, $\Delta m_{ij}^2 = m_{\nu i}^2 - m_{\nu j}^2$ is the difference of the squares of the neutrino masses, and is the Dirac-like CPV phase. The latter is the just phase associated with CPV involved in the transition amplitudes of neutrino oscillations.

PARAMETER	BFP ± 1σ	2σ range	3σ range
$\Delta m_{21}^2 : [10^{-5}\,\mathrm{eV}^2]$	$7.50^{+0.22}_{-0.20}$	7.11 – 7.93	6.94 – 8.14
$\Delta m_{31}^2 : [10^{-3}\,\mathrm{eV}^2](\mathrm{NH})$	$2.56^{+0.03}_{-0.04}$	2.49 – 2.62	2.46 – 2.65
$\Delta m_{13}^2 : [10^{-3}\,\mathrm{eV}^2](\mathrm{IH})$	2.46 ± 0.03	2.40 – 2.52	2.37 – 2.55
$\sin^2\theta_{12} / 10^{-1}$	3.18 ± 0.16	2.86 – 3.52	2.71 – 3.70
$\sin^2\theta_{23} / 10^{-1}(\mathrm{NH})$	$5.66^{+0.16}_{-0.22}$	5.05 – 5.96	4.41 – 6.09
$\sin^2\theta_{23} / 10^{-1}(\mathrm{IH})$	$5.66^{+0.18}_{-0.23}$	5.14 – 5.97	4.46 – 6.09
$\sin^2\theta_{13} / 10^{-2}(\mathrm{NH})$	$2.225^{+0.055}_{-0.078}$	2.081 – 2.349	2.015 – 2.417
$\sin^2\theta_{13} / 10^{-2}(\mathrm{IH})$	$2.250^{+0.056}_{-0.076}$	2.107 – 2.373	2.039 – 2.441
$\delta_{\mathrm{CP}} / \pi(\mathrm{NH})$	$1.20^{+0.23}_{-0.14}$	0.93 – 1.80	0.80 – 2.00
$\delta_{\mathrm{CP}} / \pi(\mathrm{IH})$	1.54 ± 0.13	1.27 – 1.79	1.14 – 1.90

The goal of Long-baseline experiments is to obtain precise measurements of neutrino oscillation parameters. In particular, the T2K, DUNE, and NOνA experiments take measurements of the transition amplitude between solar and atmospheric neutrinos, $\nu_{\mu} \to \nu_{e}$, to accurately determine the numerical value of the CPV phase Dirac-like. In the T2K experiment, the neutrino beam has a mean energy of 0.6 GeV and a width of about 0.3 GeV, traveling from the J-PARC accelerator to the Super-Kamiokande detector which is 295 km away [16]. In the NOνA experiment, the neutrino beam travels a distance of 810 km, and has an energy between 1 and 3 GeV, however, the maximum signal is around 2 GeV [17]. In the DUNE experiment, the neutrino beam is of high intensity with an average energy of 2.8 GeV, the particles travel a distance of 1300 km to the detector [18].

The neutrinoless double beta decay, $0\nu\beta\beta$, is a second-order nuclear reaction that has not yet been observed, but it makes it possible to elucidate whether the neutrinos are Dirac or Majorana particles, since only in the latter case does this decay exist. For this decay, the physical observable to be measured is the amplitude $T_{1/2}^{0\nu}$, which is sensitive to the Majorana phases associated with CP violation, and proportional to the effective Majorana mass, $\langle m_{ee}\rangle = \left|\Sigma_j m_{\nu j} U_{ej}\right|$, where the U_{ej} are elements of the PMNS matrix [19].

In this work, an independent study of models is proposed, in which the neutrinos mass terms are of Majorana type. In particular, the neutrino mass matrix form is fixed with the so-called TBM flavor pattern. On the other hand, to establish the form of the charged leptons mass matrix, an equivalence class whose elements are matrices with two texture zeros is proposed. The leptonic flavor mixing matrix, PMNS, is expressed in terms of the charged leptons masses, which allow us to obtain a deviation from the TBM standard pattern. In addition, it predicts a range of values for the Charge-Parity violation (CPV) phases and the effective Majorana mass in the neutrinoless double beta decay.

3. TBM Pattern of Matrix PMNS

The low energy neutrinos oscillations are described through the Lagrangian density [9]

$$\mathcal{L} = -\frac{g}{\sqrt{2}}\overline{\ell}_L \gamma^\mu \nu_L W_\mu + \frac{1}{2}\overline{\nu_R^c} \mathrm{M}_\nu \nu_L - \overline{\ell}_R \mathrm{M}_\ell \ell_L + \mathrm{H.c.} \quad (1)$$

The first Lagrangian term represents charged currents, M_ν is the neutrino mass matrix Majorana-like, and M_ℓ is the charged lepton mass matrix Dirac-like. In general, M_ν is a symmetric matrix, while M_ℓ has no special characteristics, both 3×3 complex matrices. These matrices are diagonalized by the following unit transformations:

$$\mathbf{M}_\nu = \boldsymbol{U}_\nu^* \, \Delta_\nu \boldsymbol{U}_\nu^\dagger, \text{ and } \mathbf{M}_\ell = \boldsymbol{V}_\ell^\dagger \Delta_\ell \boldsymbol{U}_\ell, \quad (2)$$

where $\Delta_\nu = \mathrm{diag}\left(m_{\nu 1}, m_{\nu 2}, m_{\nu 3}\right)$ and $\Delta_\ell = \mathrm{diag}\left(m_e, m_\mu, m_\tau\right)$. The unit matrices $\boldsymbol{V}_\ell$ and $\boldsymbol{U}_\ell$ are obtained by applying the singular value decomposition theorem to the charged leptons matrix $\mathbf{M}_\ell$. From (1) and (2), the charged current term takes the form $\mathcal{L}_{\mathrm{cc}} = \ell'_L \gamma^\mu \boldsymbol{U}_{\mathrm{PMNS}} \nu'_L$, where $\ell'_L = \boldsymbol{U}_\ell \ell_L$, $\nu'_L = \boldsymbol{U}_\nu \nu_L$ and $\boldsymbol{U}_{\mathrm{PMNS}} = \boldsymbol{U}_\ell^\dagger \boldsymbol{U}_\nu$ is the lepton flavor mixing matrix, known as the PMNS matrix that governs the neutrinos and leptons couplings.

In symmetric parameterization, the PMNS matrix has the form [19]:

$$\begin{pmatrix} C_{13}C_{12} & C_{13}S_{12}e^{-i\phi_{12}} & S_{13}e^{-i\phi_{13}} \\ -C_{23}S_{12}e^{-\phi_{12}} - S_{23}C_{12}S_{13}e^{-i(\phi_{23}-\phi_{13})} & C_{23}C_{12} - S_{23}S_{12}S_{13}e^{-i(\phi_{12}+\phi_{23}-\phi_{13})} & C_{13}S_{23}e^{-i\phi_{23}} \\ S_{23}S_{12}e^{i(\phi_{12}+\phi_{23})} - C_{23}C_{12}S_{13}e^{i\phi_{13}} & -S_{23}C_{12}e^{i\phi_{23}} - C_{23}S_{12}S_{13}e^{-i(\phi_{12}-\phi_{13})} & C_{13}C_{23} \end{pmatrix} \quad (3)$$

where $C_{ij} \equiv \cos\theta_{ij}$ and $S_{ij} \equiv \sin\theta_{ij}$. The symmetric and PDG standard parameterizations are related to each other through the $\boldsymbol{U}_{\mathrm{PDG}} = \boldsymbol{K}\boldsymbol{U}_{\mathrm{Sim}}$, where $\boldsymbol{K} = \mathrm{diag}\left(1, \; e^{i\frac{\beta_1}{2}}, \; e^{i\frac{\beta_1}{2}}\right)$ with $\beta_1 = -2\phi_{12}$, $\beta_2 = -2\left(\phi_{12}+\phi_{23}\right)$; $\delta_{\mathrm{CP}} = \phi_{13} - \phi_{23} - \phi_{12}$. The mixing angles in terms of the matrix PMNS entries have the following form [19, 20]:

$$\sin^2\theta_{13} = \left|\left(\boldsymbol{U}_{\mathrm{PMNS}}\right)_{13}\right|^2, \; \sin^2\theta_{12} = \frac{\left|\left(\boldsymbol{U}_{\mathrm{PMNS}}\right)_{12}\right|^2}{1-\left|\left(\boldsymbol{U}_{\mathrm{PMNS}}\right)_{13}\right|^2}, \quad \sin^2\theta_{23} = \frac{\left|\left(\boldsymbol{U}_{\mathrm{PMNS}}\right)_{23}\right|^2}{1-\left|\left(\boldsymbol{U}_{\mathrm{PMNS}}\right)_{13}\right|^2}. \quad (4)$$

These expressions are invariant before reparametrizations of the matrix PMNS. The CPV phases ϕ_{12}, ϕ_{13} and δ_{CP} have the expressions:

$$\sin^2\delta_{\mathrm{CP}} = \frac{J_{\mathrm{CP}}\left(1-\left|\left(\boldsymbol{U}_{\mathrm{PMNS}}\right)_{13}\right|\right)^2}{\left|\left(\boldsymbol{U}_{\mathrm{PMNS}}\right)_{11}\right|\left|\left(\boldsymbol{U}_{\mathrm{PMNS}}\right)_{12}\right|\left|\left(\boldsymbol{U}_{\mathrm{PMNS}}\right)_{13}\right|\left|\left(\boldsymbol{U}_{\mathrm{PMNS}}\right)_{23}\right|\left|\left(\boldsymbol{U}_{\mathrm{PMNS}}\right)_{33}\right|},$$
$$\sin\left(-2\phi_{12}\right) = \frac{I_1}{\left|\left(\boldsymbol{U}_{\mathrm{PMNS}}\right)_{11}\right|^2\left|\left(\boldsymbol{U}_{\mathrm{PMNS}}\right)_{12}\right|^2}, \; \sin(-2\phi_{13}) = \frac{I_2}{\left|\left(\boldsymbol{U}_{\mathrm{PMNS}}\right)_{11}\right|^2\left|\left(\boldsymbol{U}_{\mathrm{PMNS}}\right)_{13}\right|^2}, \quad (5)$$

where $J_{\mathrm{CP}} = Im\left\{\left(\boldsymbol{U}_{\mathrm{PMNS}}\right)_{13}\left(\boldsymbol{U}_{\mathrm{PMNS}}\right)_{23}^*\left(\boldsymbol{U}_{\mathrm{PMNS}}\right)_{11}^*\left(\boldsymbol{U}_{\mathrm{PMNS}}\right)_{21}\right\}$ is the Jarlskog invariant, associated with a CPV Dirac-like. Moreover, $I_1 = Im\left\{\left(\boldsymbol{U}_{\mathrm{PMNS}}\right)_{12}^2\left(\boldsymbol{U}_{\mathrm{PMNS}}\right)_{11}^{*2}\right\}$ and $I_2 = Im\left\{\left(\boldsymbol{U}_{\mathrm{PMNS}}\right)_{13}^2\left(\boldsymbol{U}_{\mathrm{PMNS}}\right)_{11}^{*2}\right\}$ are invariant related to CPV phases Majorana-like [19].

In order to obtain the TBM pattern in lepton flavor mixing, we should take into account that charged lepton mass matrix $\mathbf{M}_\ell$ is diagonal. Moreover, solar, atmospheric and reactor mixing angles have the values $\sin\theta_{12} = \frac{1}{\sqrt{3}}$, $\theta_{23} = \frac{\pi}{4}$, and $\theta_{13} = 0$ respectively. Further, these one preserve (CP) symmetry, whence phase factors in any parametrization must be null. Then, matrix PMNS has the form [11]

$$\boldsymbol{U}_{\text{PMNS}} = \boldsymbol{U}_{\text{TBM}} = \begin{pmatrix} \sqrt{\frac{2}{3}} & \frac{1}{\sqrt{3}} & 0 \\ -\frac{1}{\sqrt{6}} & \frac{1}{\sqrt{3}} & \frac{1}{\sqrt{2}} \\ \frac{1}{\sqrt{6}} & -\frac{1}{\sqrt{3}} & \frac{1}{\sqrt{2}} \end{pmatrix}. \tag{6}$$

In this scenario, neutrino mass matrix $\mathbf{M}_\nu$ is expressed, by considering (2) and (6), as:

$$\mathbf{M}_\nu = \begin{pmatrix} b_\nu & a_\nu & -a_\nu \\ a_\nu & b_\nu + d_\nu & b_\nu + c_\nu \\ -a_\nu & b_\nu + c_\nu & b_\nu + d_\nu \end{pmatrix}, \tag{7}$$

where $a_\nu = \frac{1}{3}(m_{\nu 2} - m_{\nu 1})$, $b_\nu = \frac{1}{3}(2m_{\nu 1} + m_{\nu 2})$, $c_\nu = \frac{1}{2}\left(m_{\nu 3} + \frac{4}{3}m_{\nu 2} + \frac{5}{3}m_{\nu 1}\right)$ and $d_\nu = \frac{1}{2}(m_{\nu 3} - m_{\nu 1})$.

However, in concordance with current experimental data of neutrino oscillations, TBM pattern is not realistic as the reactor angle θ_{13} and CPV phase δ_{CP} are non nulls.

Motivated by the need to deviate from the simplest form, to first order, for the TBM pattern (6), and considering that from a theoretical point of view, the PMNS lepton flavor mixing matrix comes from the discordance between the charged lepton mass matrix and neutrinos diagonalization, we propose a generalized version of TBM pattern. For that, neutrino mass matrix is given by (7), whereas to fix the charged lepton mass matrix form we propose several equivalence classes. These are different one and other by the texture zeros number in their matrices. Particularly, one takes that the charged lepton mass matrix is constructed through a Hermitian matrix, which in terms of an equivalence class is expressed as

$$\mathbf{M}_\ell^i = \boldsymbol{U}_\ell^i \Delta_\ell \boldsymbol{U}_\ell^{i\dagger} \tag{8}$$

where $\boldsymbol{U}_\ell^i = \boldsymbol{T}_i^\dagger \boldsymbol{P}_\ell^\dagger \boldsymbol{O}_\ell$ $(i = 0, \cdots, 6)$. Here, $\boldsymbol{T}_i$ are the elements of S_3 real representation [19, 20]. $\boldsymbol{P}_\ell$ is the diagonal matrix of phase factors, which is obtained to write down $\mathbf{M}_\ell^i$ in a polar form. Finally, $\boldsymbol{O}_\ell$ is a real and orthogonal matrix. So, matrix PMNS takes the form

$$\boldsymbol{U}_{PMNS}^i = \boldsymbol{U}_\ell^{i\dagger} \boldsymbol{U}_\nu = \boldsymbol{O}_\ell^T \boldsymbol{P}_\ell \boldsymbol{T}_i \boldsymbol{U}_{\text{TBM}}. \tag{9}$$

We fix the form of $\mathbf{M}_\ell^i$ to can obtain the explicit form of $\boldsymbol{O}_\ell$. Then, the explicit form to one equivalence class with two texture zeros is:

$$\begin{aligned} &\mathrm{M}_\ell^0 = \begin{pmatrix} 0 & a_\ell & 0 \\ a_\ell^* & b_\ell & c_\ell \\ 0 & c_\ell^* & d_\ell \end{pmatrix} \quad \mathrm{M}_\ell^1 = \begin{pmatrix} b_\ell & a_\ell^* & c_\ell \\ a_\ell & 0 & 0 \\ c_\ell^* & 0 & d_\ell \end{pmatrix} \quad \mathrm{M}_\ell^2 = \begin{pmatrix} d_\ell & c_\ell^* & 0 \\ c_\ell & b_\ell & a_\ell^* \\ 0 & a_\ell & 0 \end{pmatrix} \\ &\mathrm{M}_\ell^3 = \begin{pmatrix} 0 & 0 & a_\ell \\ 0 & d_\ell & c_\ell^* \\ a_\ell^* & c_\ell & b_\ell \end{pmatrix} \quad \mathrm{M}_\ell^4 = \begin{pmatrix} d_\ell & 0 & c_\ell^* \\ 0 & 0 & a_\ell \\ c_\ell & a_\ell^* & b_\ell \end{pmatrix} \quad \mathrm{M}_\ell^5 = \begin{pmatrix} b_\ell & c_\ell & a_\ell^* \\ c_\ell^* & d_\ell & 0 \\ a_\ell & 0 & 0 \end{pmatrix} \end{aligned} \tag{10}$$

where

$$\begin{aligned} a_\ell &= \sqrt{\frac{\tilde{m}_e \tilde{m}_\mu}{1-\delta_\ell}} e^{i\phi_a}, \\ b_\ell &= \tilde{m}_e - \tilde{m}_\mu + \delta_\ell, \\ c_\ell &= \sqrt{\frac{\delta_\ell}{1-\delta_\ell} f_{\ell 1} f_{\ell 2}} e^{i\phi_c} \end{aligned} \tag{11}$$

with, $d_\ell = 1 - \delta_\ell$, $f_{\ell 1} = 1 - \tilde{m}_e - \delta_\ell$, $f_{\ell 2} = 1 + \tilde{m}_\mu - \delta_\ell$, $\phi_a = \arg\{a_\ell\}$, $\phi_c = \arg\{c_\ell\}$, $\tilde{m}_e = \frac{m_e}{m_\tau}$, and $\tilde{m}_\mu = \frac{m_\mu}{m_\tau}$. The parameter δ_ℓ must satisfy the constraints $0 < \delta_\ell < 1 - \tilde{m}_e$ and $\delta_\ell \neq \tilde{m}_\mu - \tilde{m}_e$. In this case, phase matrix is $\boldsymbol{P}_\ell = \operatorname{diag}\left(1, \quad e^{i\phi_a}, \quad e^{i(\phi_a+\phi_c)}\right)$. The orthogonal matrix $\boldsymbol{O}_\ell$ takes the form

$$O_\ell = \begin{pmatrix} \sqrt{\frac{\tilde{m}_\mu f_{\ell 1}}{D_{\ell 1}}} & -\sqrt{\frac{\tilde{m}_e f_{\ell 2}}{D_{\ell 2}}} & \sqrt{\frac{\tilde{m}_e \tilde{m}_\mu \delta_\ell}{D_{\ell 3}}} \\ \sqrt{\frac{\tilde{m}_e (1-\delta_\ell) f_{\ell 1}}{D_{\ell 1}}} & \sqrt{\frac{\tilde{m}_\mu (1-\delta_\ell) f_{\ell 2}}{D_{\ell 2}}} & \sqrt{\frac{\delta_\ell (1-\delta_\ell)}{D_{\ell 3}}} \\ -\sqrt{\frac{\tilde{m}_e \delta_\ell f_{\ell 2}}{D_{\ell 1}}} & -\sqrt{\frac{\tilde{m}_\mu \delta_\ell f_{\ell 1}}{D_{\ell 2}}} & \sqrt{\frac{f_{\ell 1} f_{\ell 2}}{D_{\ell 3}}} \end{pmatrix}, \tag{12}$$

where $D_{\ell 1}=(1-\delta_\ell)(\tilde{m}_e+\tilde{m}_\mu)(1-\tilde{m}_e)$, $D_{\ell 2}=(1-\delta_\ell)(\tilde{m}_e+\tilde{m}_\mu)(1+\tilde{m}_\mu)$, and $D_{\ell 3}=(1-\delta_\ell)(1+\tilde{m}_\mu)(1-\tilde{m}_e)$.
From the theoretical expressions of the PMNS matrices in eq. (9), we obtain that the reactor, atmospheric, and solar mixing angles only has three different forms for an equivalent class. In particular, for $\mathbf{M}_\ell^0$ and $\mathbf{M}_\ell^3$. we have $\left|\left(\boldsymbol{U}_{PMNS}^0\right)_{13}\right|=\left|\left(\boldsymbol{U}_{PMNS}^3\right)_{13}\right|$, $\left|\left(\boldsymbol{U}_{PMNS}^0\right)_{12}\right|=\left|\left(\boldsymbol{U}_{PMNS}^3\right)_{12}\right|$, and $\left|\left(\boldsymbol{U}_{PMNS}^0\right)_{23}\right|=\left|\left(\boldsymbol{U}_{PMNS}^3\right)_{23}\right|$.

4. Numerical Results

Our main goal is found a form of $\mathbf{M}_\ell^0$ that provides a reactor angle deviation of null value, which is in TBM pattern, and at the same time, provides a current numerical values for solar and atmospheric angles. One numerical analysis is done, in which is taken into account the following values of charged lepton masses (GeV):

$$\begin{aligned} m_e &= 0.5109998928 \pm 0.000000011, \\ m_\mu &= 105.6583715 \pm 0.0000035, \\ m_\tau &= 1776.82 \pm 0.16. \end{aligned} \tag{13}$$

Then, mass ratios are $\tilde{m}_e \sim 10^{-4}$ and $\tilde{m}_\mu \sim 10^{-2}$. Parameteris δ_ℓ in the range $(0, 1-\tilde{m}_e)$, and must fulfill the condition $\delta_\ell \neq \tilde{m}_\mu - \tilde{m}_e$. The phase factors ϕ_a and ϕ_c are in the range $[-\pi, \pi]$. Finally, supported on above statement and beginning with (9), (12) and (4), first result obtained is the theoretical expression of reactor mixing angle, which more depends on ϕ_a that ϕ_c. Furthermore, the only mass matrix in the equivalence class (10) by reproducing the current experimental value of reactor angle are $\mathbf{M}_\ell^0$ and $\mathbf{M}_\ell^3$. In Figure 1 are shown the shape of the theoretical mixing angles expressions. To obtain these plots, phase factors take the numerical values $\phi_a = 0.9$ rad and $\phi_c = 1.78$ rad.

On Figure 1(a), we conclude the BFP is obtained for large values of δ_ℓ as $\delta_\ell = 0.9$, whereas solar angle can be reproduced with any value of δ_ℓ, Figure 1(b). On Figure 1(c), atmospheric angle, BFP is obtained $\delta_\ell = 0.06,\ 0.98$ (NH) and $\delta_\ell = 0.07,\ 0.99$ (IH). Then, we conclude that $\delta_\ell = 0.9$, $\phi_a = 0.9$ rad and $\phi_c = 1.78$ rad reproduce the current experimental values of the three lepton flavor mixing angles. Figure 2 show CPV phases ϕ_{12}, ϕ_{13} and δ_{CP} & δ_ℓ.

Transition probability in matter for solar and atmospheric oscillations, $\nu_\mu \to \nu_e$ and $\bar{\nu}_\mu \to \bar{\nu}_e$ respectively, can be described through the expressions [19, 20],

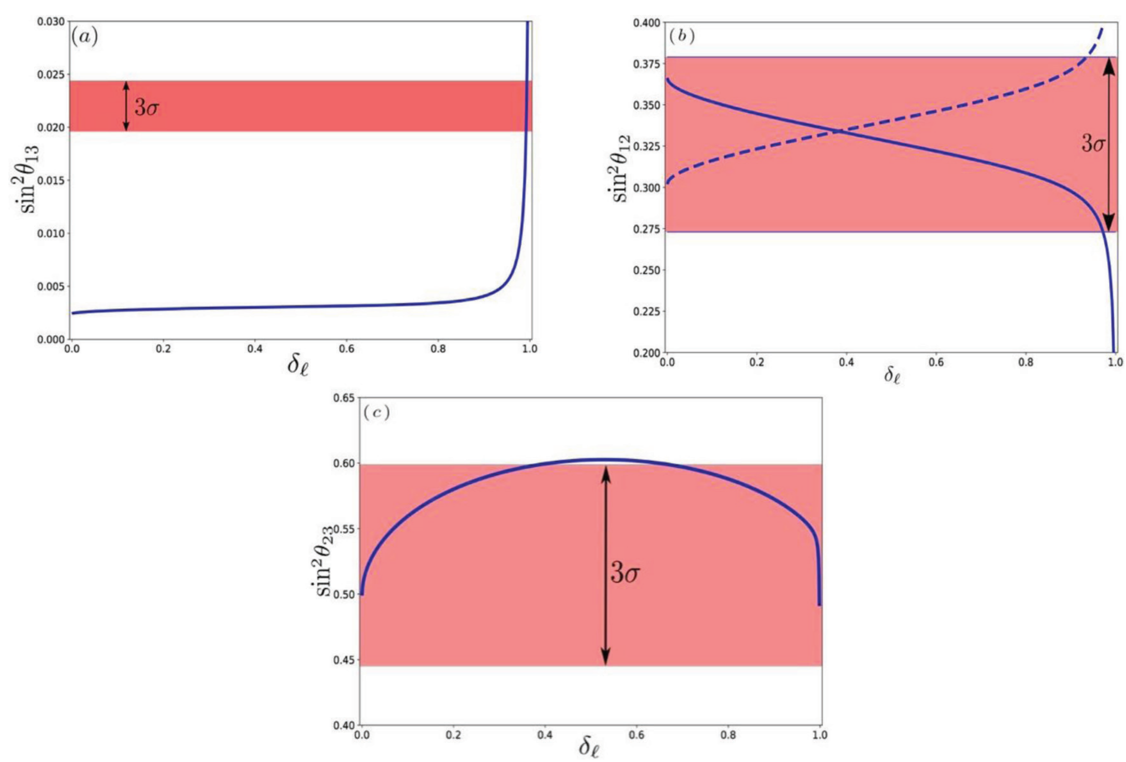

Figure 1: Respectively, the plots (a) and (b) show $\sin^2\theta_{13}$ and $\sin^2\theta_{12}$, and (c) $\sin^2\theta_{23}$ respect to δ_ℓ parameter. The red zone is the allowed experimental parameter region in range BFP $\pm 3\sigma$ (NH and IH), with $\phi_a = 0.9$ rad and $\phi_c = 1.78$ rad. The blue solid and dashed lines correspond to $\mathbf{M}_\ell^0$ and $\mathbf{M}_\ell^3$, respectively.

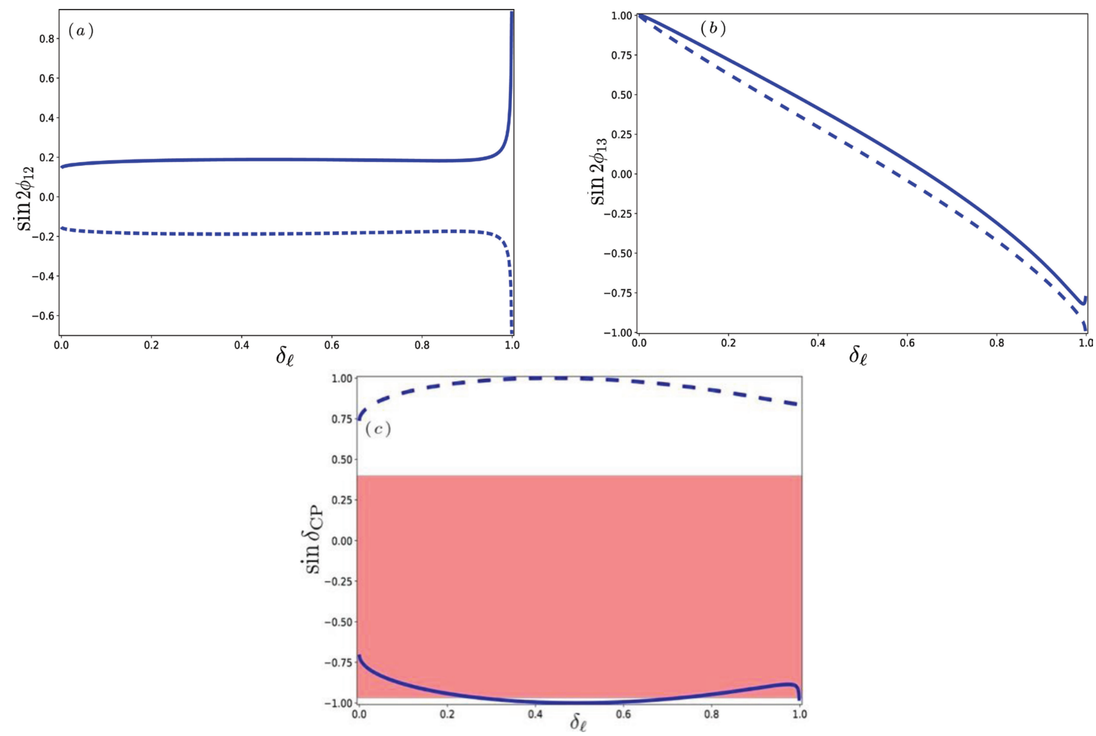

Figure 2: Plots (a) and (b) show $\sin(2\phi_{12})$ and $\sin(2\phi_{13})$ respectively, and (c) $\sin\delta_{CP}$ respect to δ_ℓ . Green zone is the allowed experimental parameter region in range $\mathrm{BFP}\pm 3\sigma$ (NH and IH), with $\phi_a = 0.9$ rad and $\phi_c = 1.78$ rad. Blue solid and orange dashed lines correspond to $\mathbf{M}_\ell^0$ and $\mathbf{M}_\ell^3$, respectively.

$$\begin{aligned} \mathrm{P}\left(\nu_\mu \to \nu_e\right) &\approx P_{\mathrm{atm}} + P_{\mathrm{sol}} + 2\sqrt{P_{\mathrm{atm}}}\sqrt{P_{\mathrm{sol}}}\sin\left(\Delta_{32}+\delta_{\mathrm{CP}}\right), \\ \mathrm{P}\left(\bar{\nu}_\mu \to \bar{\nu}_e\right) &\approx \mathcal{P}_{\mathrm{atm}} + P_{\mathrm{sol}} + 2\sqrt{\mathcal{P}_{\mathrm{atm}}}\sqrt{P_{\mathrm{sol}}}\cos\left(\Delta_{32}-\delta_{\mathrm{CP}}\right), \end{aligned} \tag{14}$$

where

$$\begin{aligned} \sqrt{P_{\mathrm{sol}}} = \cos\theta_{23}\sin 2\theta_{12}\frac{\sin aL}{aL}\Delta_{21}, \ \sqrt{P_{\mathrm{atm}}} &= \sin\theta_{23}\sin 2\theta_{13}\frac{\sin\left(\Delta_{31}-aL\right)}{\Delta_{31}-aL}\Delta_{31}, \\ \sqrt{\mathcal{P}_{\mathrm{atm}}} &= \sin\theta_{23}\sin 2\theta_{13}\frac{\sin\left(\Delta_{31}+aL\right)}{\Delta_{31}+aL}\Delta_{31}. \end{aligned} \tag{15}$$

Δ_{ij} and are expressed as $\Delta_{ij} = \dfrac{\Delta m_{ij}^2 L}{4E}$, $a = \dfrac{G_F N_e}{\sqrt{2}}$; L is the line length, E is the neutrino beam energy, N_e is the electron density and G_F is the Fermi constant. Parameter a has the value $\sim(3500\mathrm{km})^{-1}$. One can see in Figure 3 the transition probabilities $\nu_\mu \to \nu_e$ and $\bar{\nu}_\mu \to \bar{\nu}_e$, for $\mathbf{M}_\ell^0$ and $\mathbf{M}_\ell^3$. Moreover, the phase factors take the numerical values $\phi_a = 0.9\,\mathrm{rad}$ and $\phi_c = 1.78\,\mathrm{rad}$.

In the symmetric parametrization of PMNS (3), Majorana effective mass in double beta decay without neutrinos, $0\nu\beta\beta$, has the form [19, 20]:

$$\begin{aligned} \langle m_{ee}\rangle = \big| & m_{\nu 1}\cos^2\theta_{12}\cos^2\theta_{13} \\ & + m_{\nu 2}\mathrm{sen}^2\theta_{12}\cos^2\theta_{13}e^{-i2\phi_{12}} + m_{\nu 3}\mathrm{sen}^2\theta_{13}e^{-i2\phi_{13}}\big| \end{aligned} \tag{16}$$

where ϕ_{12} and ϕ_{13} are given in (5). To analyze the effective mass $\langle m_{ee}\rangle$, neutrino masses are expressed in terms of Δm_{ij}^2, and the light neutrino mass in each hierarchy of neutrino spectrum. Then,

$$m_{\nu 2} = \sqrt{\Delta m_{21}^2 + m_{\nu 1}^2} \text{ and } m_{\nu 3} = \sqrt{\Delta m_{31}^2 + m_{\nu 1}^2} \text{ (NH)}, \tag{17}$$

$$\begin{aligned} m_{\nu 1} &= \sqrt{\Delta m_{13}^2 + m_{\nu 3}^2} \text{ and} \\ m_{\nu 2} &= \sqrt{\Delta m_{13}^2 + \Delta m_{21}^2 + m_{\nu 3}^2} \text{ (IH)}. \end{aligned} \tag{18}$$

Figure 4 show $\langle m_{ee}\rangle$ & $m_{\nu,light}$ for $\mathbf{M}_\ell^0$ and $\mathbf{M}_\ell^3$, fixing $\phi_a = 0.9\,\mathrm{rad}$ and $\phi_c = 1.78\,\mathrm{rad}$.

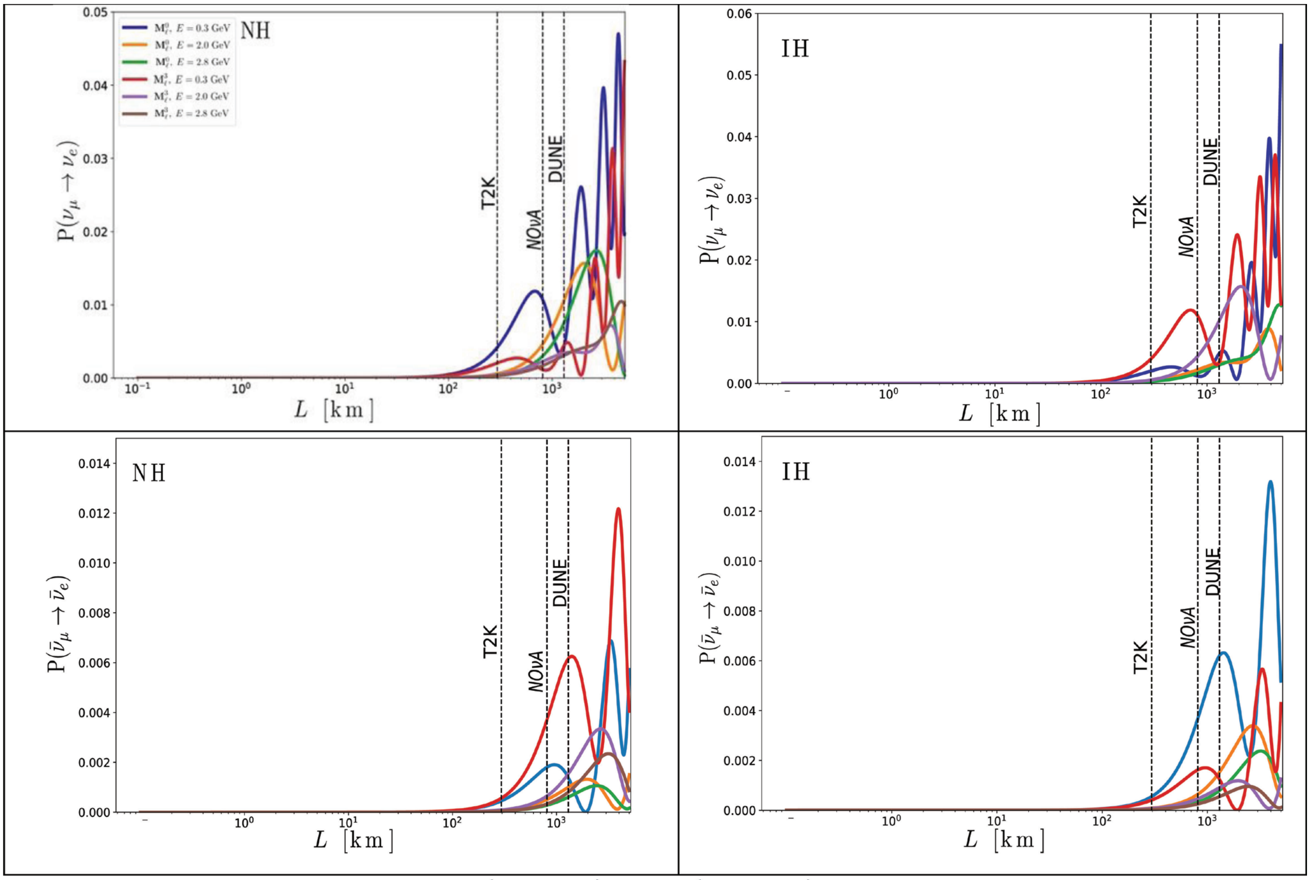

Figure 3: Transition probabilities $P(\nu_\mu \to \nu_e)$ and $P(\bar{\nu}_\mu \to \bar{\nu}_e)$ for Inverted (IH) and Normal (NH) Hierarchies. Phase factors are fixing on $\phi_a = 0.9\,\text{rad}$ and $\phi_c = 1.78$ rad. Blue, orange and green lines correspond to $\mathbf{M}_\ell^0$, with E = 0.3, 2.0, 2.8 GeV respectively. Red, purple and brown lines correspond to $\mathbf{M}_\ell^3$, for E = 0.3, 2.0, 2.8 GeV respectively.

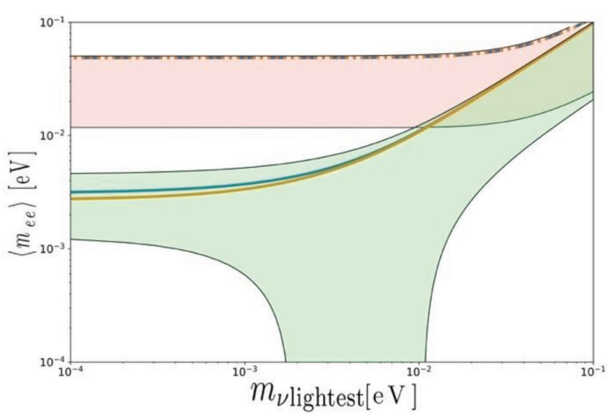

Figure 4: Majorana effective mass, $\langle m_{ee} \rangle$. Red (IH) and green (NH) zones are obtained with the current experimental data of neutrino oscillations in the range $\text{BFP} \pm 3\sigma$. Orange solid and dashed lines correspond to the prediction on $\mathbf{M}_\ell^3$. Phase factors are fixing to $\phi_a = 0.9$ rad and $\phi_c = 1.78\,\text{rad}$.

Conclusion

In theoretical frame of an independent model study, one considered that Majorana neutrino mass matrix is represented through one matrix with a mixing TBM pattern. In case of the charged lepton mass matrix, we explored six mass matrices corresponding to one equivalence class with two zeros. One obtained that just $\mathbf{M}_\ell^0$ and $\mathbf{M}_\ell^3$, reproduced the current numerical values of mixing angles. Moreover, we obtain that the reactor, atmospheric, and solar mixing angles just have three different forms for an equivalent class. Furthermore, one can obtained predictions for CPV phases like-Dirac and Majorana as well. Likewise, phenomenological implications were shown for the DUNE, T2K and NOνA experiments. Finally, a numerical range values is provided for the Majorana effective mass in the double beta decay without neutrinos.

References

[1] C.L. Cowan, F. Reines, F.B. Harrison, H.W. Kruse and A.D. MacGuire, Science **124**, 103 (1956). https://doi.org/10.1126/science.124.3212.103

[2] S.P. Carpi, *Los neutrinos*. Consejo Superior de Investigación Científica; Los libros de la Catarata, Madrid, España, p. 1-128. (2014).

[3] J.N. Bahcall and R. Davis, Science **191**, 264 (1976). https://doi.org/10.1126/science.191.4224.264

[4] S. Fukuda, et al., Nucl. Instrum. Meth. Phys. Res. A **501**, 418 (2003). https://doi.org/10.1016/S0168-9002(03)00425-X

[5] Q.R. Ahmad, et al. (SNO Collaboration), Phys. Rev. Lett. **87**, 071301 (2001). https://doi.org/10.1103/PhysRevLett.87.071301

[6] A. Bellerive, et al. (SNO Collaboration), Nucl. Phys. B **908**, 30 (2016). https://doi.org/10.1016/j.nuclphysb.2016.04.035

[7] S. Adrián-Martínez, et al. (ANTARES Collaboration), Phys. Lett. B **714**, 224 (2012). https://doi.org/10.1016/j.physletb.2012.07.002

[8] A. Salam, Conf. Proc. C **680519**, 367 (1968).; S. Weinberg, Phys. Rev. Lett. **19,** 1264 (1967). https://doi.org/10.1103/PhysRevLett.19.1264; S.L. Glashow, Nucl. Phys. **22**, 579 (1961). https://doi.org/10.1016/0029-5582(61)90469-2

[9] P.A. Zyla, et al. (Particle Data Group), Prog. Theor. Exp. Phys. **2020**, 083C01 (2020).

[10] A.B. Balantekin, A. de Gouvea and B. Kayser, Phys. Lett. B **789**, 488 (2018). https://doi.org/10.1016/j.physletb.2018.11.068

[11] P.F. Harrison, D.H. Perkins and W.G. Scott, Phys. Lett. B **530**, 167 (2002). https://doi.org/10.1016/S0370-2693(02)01336-9

[12] V. Barger, S. Pakvasa, T.J. Weiler and K. Whisnant, Phys. Lett. B **437**, 107 (1998). https://doi.org/10.1016/S0370-2693(98)00880-6

[13] H. Fritzsch and Z.-Z. Xing, Phys. Lett. B **372**, 265 (1996). https://doi.org/10.1016/0370-2693(96)00107-4

[14] K. Abe, et al. (T2K Collaboration), Phys. Rev. Lett. **107**, 041801 (2011). https://doi.org/10.1103/PhysRevLett.107.041801

[15] F.P. An, et al. (DAYA-BAY Collaboration), Phys. Rev. Lett. **108**, 171803 (2012). https://doi.org/10.1103/PhysRevLett.108.171803

[16] P.F. de Salas, D.V. Forero, S. Gariazzo, P. Martínez-Miravé, O. Mena, M. Tortola and J.W.F. Valle, [ArXiv:hep-ph/2006.11237].

[17] P. Adamson, et al. (NOVA Collaboration), Phys. Rev. D **93**, 051104 (2016). https://doi.org/10.1103/PhysRevD.93.051104

[18] B. Abi, et al. (DUNE Collaboration), [ArXiv:1807.10334].

[19] P. Chen, G.-J. Ding, F. González-Canales and J.W.F. Valle, Phys. Lett. B **753**, 644 (2016). https://doi.org/10.1016/j.physletb.2015.12.069

[20] W. Rodejohann and J.W.F. Valle, Phys. Rev. D **84**, 073011 (2011). https://doi.org/10.1103/PhysRevD.84.073011; E. Barradas-Guevara, O. Félix-Beltrán, F. González-Canales and M. Zeleny-Mora, Phys. Rev. D **97,** 035003 (2018). https://doi.org/10.1103/PhysRevD.97.035003

CHITKARA

Journal of Nuclear Physics, Material Sciences, Radiation and Applications

Chitkara University, Saraswati Kendra, SCO 160-161, Sector 9-C, Chandigarh, 160009, India

Volume 8, Issue 2 **February 2021** **ISSN 2321-8649**